



Published in final edited form as:

*Kidney Int.* 2018 December ; 94(6): 1127–1140. doi:10.1016/j.kint.2018.06.025.

## CD8<sup>+</sup> T cells modulate autosomal dominant polycystic kidney disease progression

Emily K. Kleczko<sup>1</sup>, Kenneth H. Marsh<sup>1</sup>, Logan C. Tyler<sup>1</sup>, Seth B. Furgeson<sup>1,2</sup>, Bonnie L. Bullock<sup>1</sup>, Christopher J. Altmann<sup>1</sup>, Makoto Miyazaki<sup>1</sup>, Berenice Y. Gitomer<sup>1</sup>, Peter C. Harris<sup>3</sup>, Mary C.M. Weiser-Evans<sup>1,2</sup>, Michel B. Chonchol<sup>1,2</sup>, Eric T. Clambey<sup>4</sup>, Raphael A. Nemenoff<sup>1,2</sup>, and Katharina Hopp<sup>1,2</sup>

<sup>1</sup>Department of Medicine, Division of Renal Diseases and Hypertension, University of Colorado Anschutz Medical Campus, Aurora, Colorado, USA

<sup>2</sup>Consortium for Fibrosis Research and Translation, University of Colorado Anschutz Medical Campus, Aurora, Colorado, USA

<sup>3</sup>Department of Medicine, Division of Nephrology and Hypertension, Mayo Clinic, Rochester, Minnesota, USA

<sup>4</sup>Department of Anesthesiology, University of Colorado Anschutz Medical Campus, Aurora, Colorado, USA

### Abstract

Autosomal dominant polycystic kidney disease (ADPKD) is the most prevalent inherited nephropathy. To date, therapies alleviating the disease have largely focused on targeting abnormalities in renal epithelial cell signaling. ADPKD has many hallmarks of cancer, where targeting T cells has brought novel therapeutic interventions. However, little is known about the role and therapeutic potential of T cells in ADPKD. Here, we used an orthologous ADPKD model, *Pkd1* p.R3277C (RC), to begin to define the role of T cells in disease progression. Using flow cytometry, we found progressive increases in renal CD8<sup>+</sup> and CD4<sup>+</sup> T cells, correlative with disease severity, but with selective activation of CD8<sup>+</sup> T cells. By immunofluorescence, T cells specifically localized to cystic lesions and increased levels of T-cell recruiting chemokines (CXCL9/CXCL10) were detected by qPCR/*in situ* hybridization in the kidneys of mice, patients, and ADPKD epithelial cell lines. Importantly, immunodepletion of CD8<sup>+</sup> T cells from one to three months in C57Bl/6 *Pkd1*<sup>RC/RC</sup> mice resulted in worsening of ADPKD pathology, decreased apoptosis, and increased proliferation compared to IgG-control, consistent with a reno-protective role of CD8<sup>+</sup> T cells. Thus, our studies suggest a functional role for T cells, specifically CD8<sup>+</sup> T

---

This is an open access article under the CC BY-NC-ND license (<http://creativecommons.org/licenses/by-nc-nd/4.0/>).

**Correspondence:** Katharina Hopp, Division of Renal Diseases & Hypertension, University of Colorado Anschutz Medical Campus, 12700 E 19th Avenue, P15-7400A, Mail Stop C281, Aurora, Colorado 80045, USA. [Katharina.hopp@ucdenver.edu](mailto:Katharina.hopp@ucdenver.edu); or Raphael A. Nemenoff, Division of Renal Diseases & Hypertension, University of Colorado Anschutz Medical Campus, 12700 E 19<sup>th</sup> Avenue, P15-7100, Mail Stop C281, Aurora, Colorado 80045, USA. [Raphael.nemenoff@ucdenver.edu](mailto:Raphael.nemenoff@ucdenver.edu).

#### DISCLOSURE

All the authors declared no competing interests.

Supplementary methods.

Supplementary material is linked to the online version of the paper at [www.kidney-international.org](http://www.kidney-international.org).

cells, in ADPKD progression. Hence, targeting this pathway using immune-oncology agents may represent a novel therapeutic approach for ADPKD.

### Keywords

adaptive immunity; autosomal dominant polycystic kidney disease; CD8<sup>+</sup> T cells; *Pkd1* RC mouse model

Autosomal dominant polycystic kidney disease (ADPKD) is the most common, potentially lethal monogenic nephropathy caused predominantly by mutations to either *PKD1* or *PKD2*.<sup>1-4</sup> ADPKD accounts for 8% to 10% of patients receiving renal replacement therapy for end-stage renal disease (ESRD) worldwide<sup>5</sup> and affects roughly 1:400 to 1:1000 people.<sup>6,7</sup> The disease is characterized by dysregulated growth of renal epithelial cells leading to progressive, bilateral fluid-filled renal cysts and resulting in ESRD in about 50% of patients by middle age.<sup>8,9</sup> Extrarenal manifestations, such as liver and pancreatic cysts or cardiovascular abnormalities, further decrease quality of life and increase morbidity and mortality.<sup>10,11</sup> Previous research focused on targeting pathways central to cyst pathology, such as cyclic adenosine monophosphate/protein kinase A, epidermal growth factor, and mammalian target of rapamycin,<sup>12</sup> have provided positive data in murine preclinical trials, but their efficacy in humans was modest at best.<sup>13-17</sup> Hence the number of US Food and Drug Administration (FDA)-approved compounds for the treatment of ADPKD are limited, and ESRD is managed by either dialysis or kidney transplant.<sup>18</sup> Thus an urgent need exists to explore new treatment options that can slow the progression of ADPKD and prevent advancement to ESRD.

Whereas mutations in *PKD1* or *PKD2* mediate ADPKD initiation and progression,<sup>19,20</sup> observed intra- and interfamilial phenotypic heterogeneity, ranging from *in utero* onset<sup>21,22</sup> to adequate renal function at old age,<sup>23</sup> exceeds genic effects,<sup>3,24</sup> suggesting that additional, nongenetic factors contribute to disease progression. Further, the functional role of the *PKD1* and *PKD2* proteins, polycystin-1 and polycystin-2, while extensively studied, remains elusive, leaving many open questions regarding the mechanisms that drive cystogenesis.<sup>25-28</sup>

Although ADPKD historically has been considered a “neoplasia in disguise,”<sup>29</sup> the significant similarities between ADPKD and cancer have been rediscovered more recently.<sup>30</sup> In fact, many of the cancer hallmarks as defined by Hanahan and Weinberg<sup>31</sup> are applicable to ADPKD (e.g., sustained proliferation,<sup>12,30,32</sup> genomic instability,<sup>33-35</sup> deregulated cellular energetics,<sup>36,37</sup> and inflammation/avoiding immune destruction<sup>38-47</sup>). Importantly, interstitial inflammation has been reported in human patients with ADPKD, as well as in animal models of the disease.<sup>40</sup> In concordance with an inflammatory response, increased levels of pro-inflammatory cytokines, such as monocyte chemoattractant protein-1 and tumor necrosis factor- $\alpha$ , were detected in cyst fluid of patients with ADPKD, and anti-inflammatory therapies have been shown to attenuate disease progression in animal models.<sup>38-40</sup> Furthermore, macrophage infiltration can be observed in orthologous and nonorthologous ADPKD models at advanced disease stage,<sup>41-43</sup> and a few reports show CD4<sup>+</sup> T cells, mast cells, and neutrophils in the interstitium of patients with ADPKD.<sup>44-46</sup> Additionally, historic data showed that murine PKD models raised in germ-free

environments present with milder cystic disease,<sup>47</sup> suggesting a role for the immune system in PKD. In fact, it was shown that M2-like macrophages can promote cyst growth in murine models of autosomal recessive PKD (ARPKD) and ADPKD and that their depletion slows renal and hepatic cystogenesis.<sup>41,42,48</sup> However, to date, no research in the literature addresses the role of the adaptive immune system in ADPKD initiation and progression.

Targeting adaptive immunity has become a central focus in developing new therapeutic approaches in multiple malignancies.<sup>49,50</sup> In many cancers, increased numbers of tumor-infiltrating T cells are associated with better prognosis,<sup>51</sup> consistent with a role for these cells in inhibiting tumor progression. However, the role of different T-cell subtypes is complex because of their heterogeneity.<sup>52</sup> As such, different populations have either pro-tumorigenic (e.g., regulatory T cells [Tregs]) or antitumorigenic (e.g., CD8<sup>+</sup> T cell) roles. Additionally, cancers have developed multiple cellular and molecular pathways to suppress T-cell functions. Strategies targeting the interaction of specific T cells with cancer cells have shown recent clinical success, leading to FDA approval of checkpoint inhibitors that target the interactions of programmed cell death protein-1 (PD-1) with its ligand PD-L1, resulting in reactivation of antitumor CD8<sup>+</sup> T cells.<sup>53,54</sup> The progress made in the field of cancer research, specifically the function of T cells in tumorigenesis, may yield new ideas and avenues for ADPKD research. Thus, an essential first step forward is to understand the role of T cells in ADPKD progression.

Here, we characterized T-cell subpopulations in an orthologous mouse model of ADPKD that reproduces critical features of the human disease, including a slow rate of progression. We found that T cells increase in correlation with disease severity and localize specifically to cystic lesions. Importantly, our results define a functional role for CD8<sup>+</sup> T cells in inhibiting ADPKD progression, highlighting the potential to adapt cancer immunotherapy strategies to ADPKD.

## RESULTS

### Renal T-cell numbers are increased in the C57Bl/6 *Pkd1*<sup>RC/RC</sup> model compared with wild type

The homozygous *Pkd1* p.R3277C (*Pkd1*<sup>RC/RC</sup>)<sup>55</sup> model genetically and physiologically mimics human ADPKD. It harbors a knock-in mutation that mimics a hypomorphic allele identified in ADPKD families<sup>56</sup> and presents over time in the C57Bl/6 background with slowly progressive disease with moderate increases in percent kidney weight/body weight (%KW/BW), renal cystic/fibrotic area (index), chronic inflammation (increased renal interleukin-6/decreased interleukin-10 levels), as well as mild renal function decline (Supplementary Figure S1; Supplementary Table S1). To evaluate how the cystic microenvironment (CME), specifically T cells, differ between C57Bl/6 wild type (WT) and *Pkd1*<sup>RC/RC</sup> mice and to correlate changes in the adaptive immune system profile with cystogenesis progression, we used flow cytometry analysis of renal single cell suspensions and analyzed mice at 3, 6, and 9 months of age. In *Pkd1*<sup>RC/RC</sup> C57Bl/6 mice at 3 and 6 months, when the cystic disease is mild/moderate, respectively, we detected a statistically significant increase in immune cells (CD45<sup>+</sup>) and T cells (T-cell receptor  $\beta^+$  [TCR $\beta^+$ ]) in *Pkd1*<sup>RC/RC</sup> compared with WT mice, but the most striking increase occurred at 9 months of

age, the investigated time point at which PKD is most severe (Figure 1a and b; Supplementary Figure S1; Supplementary Table S1). The same pattern was observed for both cytotoxic T cells (CD8<sup>+</sup>) and helper T cells (CD4<sup>+</sup>, Figure 1c and d; Supplementary Table S1). Importantly, as shown by immunofluorescence, T cells (CD3<sup>+</sup>, CD4<sup>+</sup>, CD8<sup>+</sup>) specifically localized around cystic lesions even at mild stages of cystogenesis (3 months) when the global increase of T-cell number in the kidney was modest (Figure 1e and f; Supplementary Figure S2). At 9 months a more diffuse increase of T cells was notable by immunofluorescence, characterized by increased localization to noncystic areas, likely accounting for the striking increase in T-cell number at 9 months observed by flow cytometry (Figure 1b and e). This finding likely reflects the adaptive immune system's response to increasing tubular atrophy and interstitial expansion/inflammation that can be observed in 9-month-old *Pkd1*<sup>RC/RC</sup> C57Bl/6 mice, despite the slowly progressive/mild disease (Supplementary Figure S1C). Importantly, the increase in T-cell numbers between C57Bl/6 WT and *Pkd1*<sup>RC/RC</sup> mice was specific to kidney disease, as no changes were observed in spleens (Supplementary Figure S3).

### Increases in T-cell numbers correlate with PKD severity

The *Pkd1*<sup>RC/RC</sup> model presents with varying disease severity in different mouse strains, being mildest in the C57Bl/6 and significantly more severe in the 129/S6 and Balb/c backgrounds as measured by percent kidney weight/body weight, renal cystic/fibrotic area (index), renal function, and cytokine levels (Supplementary Figure S1; Supplementary Table S1). Interestingly, among these strains, only renal cyst size but not cyst number varies significantly, suggesting that variances in the rate of cyst progression rather than cyst initiation drive disease severity differences, indicative of a microenvironmental role in disease pathology (Supplementary Figure S1F and G).

To evaluate whether T-cell number increases correlate to disease severity, we performed comparable experiments in 129/S6 and Balb/c *Pkd1*<sup>RC/RC</sup> mice as for the C57Bl/6 background. We observed similar changes in the adaptive immune system in 129/S6 and Balb/c *Pkd1*<sup>RC/RC</sup> mice (Figure 2; Supplementary Figure S4). However, the overall increase in CD45<sup>+</sup> and T-cell subpopulations (TCRβ<sup>+</sup>, CD8<sup>+</sup>, and CD4<sup>+</sup>) compared with WT was much larger in the 129/S6 and Balb/c *Pkd1*<sup>RC/RC</sup> models than in the C57Bl/6 *Pkd1*<sup>RC/RC</sup> model, correlating with the more severe disease in these strains. This outcome was notable by flow cytometry (Figure 2a–d; Supplementary Figure S4; Supplementary Table S1), as well as by immunofluorescence (Figure 2e; Supplementary Figures S2 and S4; Supplementary Table S1).

### T-cell recruiting cytokines/chemokines are upregulated in ADPKD

To evaluate the rise in T-cell numbers mechanistically, we performed quantitative polymerase chain reaction for interferon (IFN)-γ, a cytokine produced by activated T cells,<sup>57</sup> and T-cell recruiting chemokines (*Cxcl9*, *Cxcl10*<sup>58,59</sup>). Levels of all 3 gene products were increased in the kidney as disease progressed (Figure 3a–c; Supplementary Table S1). In cancer, CXCL9 and CXCL10 induce lymphocyte infiltration and lead to suppression of tumor growth because of the infiltration of primarily CD8<sup>+</sup> and Th<sub>1</sub> CD4<sup>+</sup> T cells.<sup>60,61</sup> Upon further investigation, *in situ* hybridization of Balb/c *Pkd1*<sup>RC/RC</sup> renal sections revealed that

*Cxcl9/Cxcl10* are produced primarily in cystic regions, and co-immunofluorescence staining for CD3 showed that T cells co-localize near the cystic regions that produce *Cxcl9/Cxcl10* (Figure 3d). From a closer examination of these data, it is apparent that while multiple cells may be producing these chemokines, significant numbers of epithelial cells stained positive, highlighting that the cystic epithelium plays an active role in T-cell recruitment (Figure 3d, inset).

To determine if this mechanism of T-cell recruitment is relevant to human disease, we performed *in situ* hybridization for *CXCL9* and *CXCL10* on human ESRD ADPKD and ARPKD formalin-fixed-paraffin-embedded kidneys. As in mice, CD3<sup>+</sup> T cells co-localized to regions with high *CXCL9/CXCL10* levels, and both of these chemokines were produced by the cystic epithelium (Figure 3e). In both ADPKD and ARPKD, we observed similar increases in *CXCL9/CXCL10* levels and overall T-cell infiltrate to cystic regions, which were significantly higher compared with normal human kidney tissue.

Because *CXCL9/CXCL10* production by cancer cells has been reported previously and predicts tumor outcome,<sup>62,63</sup> we wanted to determine if renal epithelial cells can produce *CXCL9* and *CXCL10* *in vitro*. Using quantitative polymerase chain reaction on normal renal cortical tubular epithelial (RCTE)<sup>64</sup> cells (WT for *PKD1/PKD2*) and 9-12<sup>64</sup> cells (*PKD1* null) treated with recombinant human IFN- $\gamma$  for 24 hours, we were able to show an increase of *CXCL9* and *CXCL10* mRNA (Figure 4a and b). Interestingly, 9-12 cells had a significantly higher basal level of both cytokines compared with RCTE cells (Figure 4a and b). IFN- $\gamma$  has previously been shown to have antiproliferative effects on cancer cells via a signal transducer and activator of transcription 1 mechanism.<sup>65,66</sup> To explore whether IFN- $\gamma$  has antiproliferative effects on the ADPKD cystic epithelium, RCTE and 9-12 cells were treated with IFN- $\gamma$  for 72 hours and cell proliferation was assessed by cell count. The 9–12 cells showed decreased rates of proliferation, whereas there was no effect on normal RCTE cells (Figure 4c), suggesting that IFN- $\gamma$  produced by T cells can inhibit cyst growth by directly acting on cystic epithelial cells.

### CD8<sup>+</sup> T cells are predominantly activated in *Pkd1*<sup>RC/RC</sup> mice

We next examined cell-surface markers of T-cell activation (CD44 [expressed after antigen exposure and a switch from naive to effector or memory T cells]<sup>67</sup> and CD69 [expressed after antigen interaction]<sup>68</sup>) to better understand which T-cell subtype may play a predominant role in cystogenesis. We detected significant increases in activated CD8<sup>+</sup> but not CD4<sup>+</sup> T cells in C57Bl/6 *Pkd1*<sup>RC/RC</sup> mice compared with WT (Figure 5; Supplementary Table S1), suggesting a more prominent role of CD8<sup>+</sup> T cells in ADPKD progression. Similarly, CD8<sup>+</sup> T-cell activation also correlated with disease severity and was more pronounced in the faster progressing 129/S6 and Balb/c *Pkd1*<sup>RC/RC</sup> mice compared with the C56Bl/6 *Pkd1*<sup>RC/RC</sup> model (Figure 5; Supplementary Table S1).

Interestingly, in WT mice, we detected fewer renal CD45<sup>+</sup> and TCR $\beta$ <sup>+</sup> cells in strains with more severe disease when harboring the *Pkd1* p.R3277C mutation (129/S6 or Balb/c vs. C57Bl/6, Supplementary Figure S5A). Furthermore, C57Bl/6 mice had significantly higher levels of CD8<sup>+</sup> T cells compared with the other 2 strains, whereas the numbers of CD4<sup>+</sup> T cells were similar in all 3 strains (Supplementary Figure S5B and C). Previous studies have

documented differences in the immune system profile between C57Bl/6 and Balb/c strains, and these differences partially accounted for the variable responses to infection.<sup>69,70</sup> Hence, the difference in CD8<sup>+</sup> T cells between WT strains may partially explain the variation in severity of ADPKD across the different strains of *Pkd1*<sup>RC/RC</sup> mice.

### CD8<sup>+</sup> T cells play an anticystogenic role in ADPKD

In cancer models, activated CD8<sup>+</sup> T cells constrain tumor growth. Based on the predominant activation of CD8<sup>+</sup> T cells, the observed increase of IFN- $\gamma$  correlative with their activation, and their lower numbers in strains with more severe disease, we hypothesized that depleting this population would result in enhanced disease severity. We therefore tested this hypothesis initially in the C57Bl/6 strain, in which an increase in cystogenesis would be easier to detect compared with the more severe models, using antibody depletion. We depleted CD8<sup>+</sup> T cells twice a week by i.p. injection of anti-CD8 antibody (control: IgG) into C57Bl/6 *Pkd1*<sup>RC/RC</sup> mice from 1 to 3 months. Even though CD8<sup>+</sup> depletion was incomplete after 3 weeks of treatment (Supplementary Figure S6), 3-month-old *Pkd1*<sup>RC/RC</sup> anti-CD8–treated mice showed increased disease burden by gross kidney anatomy and histology, a significant increase in percent kidney weight/body weight, fibrotic index, and cyst size, but no change in cyst number (Figure 6a–f; Supplementary Table S2; blood urea nitrogen and plasma creatinine levels were not significantly altered). Interestingly, anti-CD8–treated mice presented with a significant decrease in terminal deoxynucleotidyltransferase–mediated dUTP nick end-labeling (TUNEL) positive cells and a significant increase in proliferating cell nuclear antigen (PCNA) positive cells within the dilated/cystic epithelium (Figure 6g–j), supporting our *in vitro* RCTE versus 9–12 IFN- $\gamma$  stimulated cell counting experiment (Figure 4c). Hence these data support a functional role for CD8<sup>+</sup> T cells in inhibiting fibrosis and ADPKD cyst progression through increasing apoptosis/decreasing proliferation, but not cyst initiation. Follow-up experiments showed that anti-CD8 depletion in the rapidly progressive 126/S6 *Pkd1*<sup>RC/RC</sup> model did not affect disease progression (Supplementary Table S2). This finding may be due to fundamental strain differences such as lower basal numbers in CD8<sup>+</sup> T-cell numbers, or it may be a related consequence of more rapidly progressing cysts altering the CME composition, resulting in diminished interactions with the adaptive immune system.

### The microenvironment of early-onset compared with typical adult-onset ADPKD is predominantly characterized by an increase in macrophages

Lastly, we examined changes in immune cells in an early-onset ADPKD model. *In utero* or early-onset ADPKD occurs in <3% of ADPKD cases and genetically is often associated with a complex *PKD1/PKD2* genotype.<sup>18</sup> To mimic this, we used the C57Bl/6 *Pkd1* p.R3277C model crossed with the C57Bl/6 *Pkd1* del2 model<sup>71</sup> (*Pkd1*<sup>RC/-</sup>), which presents with rapidly progressive cystogenesis leading to death at approximately postnatal day 25<sup>55</sup> compared with the *Pkd1*<sup>RC/RC</sup> model, which, dependent on the strain, may die at 12 months or older. At postnatal day 20, we analyzed the adaptive immune system as previously described. We noted, as with the *Pkd1*<sup>RC/RC</sup> model, an overall increase in immune cells; however, this increase was 2.3-fold more pronounced, likely correlating with increased disease severity (Figure 7a). Interestingly, the CME profile was strikingly different between both models. Whereas T-cell numbers increased in both (Figure 7b), the *Pkd1*<sup>RC/-</sup> CME was



highly inflamed, as characterized by a marked increase in macrophages (CD64<sup>+</sup>; Figure 7c). This increase predominantly drove the overall increase in CD45<sup>+</sup> cells, as evident by the contribution of macrophages to the CD45<sup>+</sup> cell population being significantly increased and the contribution of T cells decreased (Figure 7d and e). This striking increase in macrophages suggests a potential key role of this cell type in rapidly progressive disease, as previously reported in other rapidly progressive PKD models used for preclinical trials.<sup>41,42</sup> It also is characteristic of a highly inflamed microenvironment, which has been associated with more severe human disease, characterized by lower renal function and higher total kidney volume compared with typical ADPKD.<sup>72,73</sup> Correlatively, macrophage numbers have been shown to increase by histology in patients with ARPKD or advanced ADPKD<sup>42,74</sup>; however, detailed analyses at different ADPKD stages are lacking.

## DISCUSSION

Therapeutic strategies in ADPKD have largely focused on targeting dysregulated growth pathways in cystic epithelial cells, which are presumably the direct consequence of mutations in the *PKD1* or *PKD2* genes. This is analogous to targeted therapies directed against oncogenic drivers in cancer. However, in cancer, it has become clear that progression of tumors does not only involve oncogenic signaling pathways but also entails complex interactions between the cancer cells and the surrounding tumor microenvironment. It has been suggested that similar interactions are important in ADPKD progression.<sup>30</sup>

The results of our study demonstrate, for the first time, changes in adaptive immune cell populations and a functional role for CD8<sup>+</sup> T cells in ADPKD progression. Using an orthologous mouse model that mimics the slowly progressive disease of humans, we identified a rise in both renal CD8<sup>+</sup> and CD4<sup>+</sup> T cells that correlated with disease severity, with predominant activation of CD8<sup>+</sup> T cells. Importantly, even at mild stages of disease when the observed rise in T-cell numbers, as measured by flow cytometry, were modest, T cells specifically localized to cystic lesions and only increased in the kidney, suggesting that specific interactions between the cystic epithelium and T cells results in recruitment and activation of T cells. Our data support a model where T-cell recruitment occurs as a secondary event to cyst initiation/progression, presumably as a result of neoantigen presentation caused by genomic instability within the cystic epithelium.<sup>33,34</sup> Rapidly advancing cyst growth, as observed in the 129/S6 or Balb/c *Pkd1*<sup>RC/RC</sup> mice, likely is associated with an overall greater instance of genomic instability, upregulation of the neoantigen presentation pathway, and hence increased T-cell recruitment/CD8<sup>+</sup> T-cell activation, as our data confirm. Recruited/activated T cells secrete IFN- $\gamma$ , resulting in increased production of CD8<sup>+</sup> T-cell attracting chemokines (CXCL9/10) by cells within the CME and the cystic epithelium, causing further recruitment of CD8<sup>+</sup> T cells in a positive feedback loop. This ultimately reflects the adaptive immune system's attempt to eliminate cystic epithelia and suggests an anticystogenic role for CD8<sup>+</sup> T cells. We confirmed *CXCL9/CXCL10* production by CME cells and the tubular epithelium in ADPKD/ARPKD patient samples and show *in vivo* that CD8<sup>+</sup> T cells halt cyst progression by modulating tubular apoptosis and proliferation.

However, as has been shown in cancer,<sup>75</sup> recruited T cells may not always be fully capable of eliminating cyst growth because of simultaneous activation of immunosuppressive pathways, which inhibit the function of anti-tumor CD8<sup>+</sup> cells. This may explain the continuous growth of cysts even as CD8<sup>+</sup> T-cell numbers increase. Targeting these immunosuppressive pathways can result in reactivation of T cells and immunoelimination of tumors.<sup>76,77</sup> One such pathway is the immune checkpoint PD-1/PD-L1,<sup>76</sup> where PD-1 is expressed on activated T cells and PD-L1 is expressed on other cell types (epithelial cells, cancer cells, and inflammatory cells).<sup>78</sup> Binding of PD-L1 to PD-1 inactivates T-cell responses and leads to an exhausted phenotype. Treatment with blocking antibodies results in reactivation of T cells.<sup>50,79</sup> This approach has resulted in FDA approval of checkpoint inhibitors in multiple types of cancer. While repurposing of FDA-approved checkpoint inhibitors to ADPKD may not be achievable immediately because of known renal toxicities,<sup>80</sup> it is important to note that in multiple clinical cancer trials, checkpoint inhibitors have shown lasting tumor elimination even after stopping therapy.<sup>81,82</sup> Thus modifications to dosage/treatment protocols using these agents may be feasible for ADPKD, where prolonged efficacy is needed.

Our data further highlight that caution is warranted when choosing an ADPKD model to study the common, slow-progressing adult-onset form. For example, we observed that CD8<sup>+</sup> T-cell depletion did not promote cystogenesis in the rapidly progressive 129/S6 *PkdI*<sup>RC/RC</sup> mice as it did in the C57/B16 *PkdI*<sup>RC/RC</sup> model. This outcome may occur because the rapidly advancing disease leads to activation/deactivation of different pathways compared with slowly progressive disease or because differences in the CME, for example, the notably low CD8<sup>+</sup> T-cell numbers in 129/S6 mice, blunt various therapeutic approaches. Correlatively, in rapidly progressing mouse models mimicking early-onset ADPKD, it appears that changes in inflammatory cells, for example, macrophages, are more robust than changes in T cells, whereas in the slower progressing model, T cells appear to predominate. This finding could reflect the time required to develop a mutational burden that results in neoantigens recognized by the adaptive immune system. Further, our data do not show a significant increase in renal macrophages at 3 months of age in C57Bl/6 *PkdI*<sup>RC/RC</sup> mice (Figure 7), as has been published for other rapidly progressive models<sup>41,42</sup>; however, further time points and the other strains need to be studied to clearly determine whether renal macrophages rise in the *PkdI*<sup>RC/RC</sup> model. Thus, when wanting to test the translatability of immunotherapeutic approaches to alleviate typical ADPKD, choice of model will be critical.

More research will need to be performed to better elucidate the significance of increased CD4<sup>+</sup> T-cell numbers observed in our models. Currently it is difficult to predict the potential functional impact resulting from this increase because CD4<sup>+</sup> T cells have multiple subtypes (Tregs, Th<sub>1</sub>, Th<sub>2</sub>, Th<sub>17</sub>) with opposing effects on effector CD8<sup>+</sup> T-cell function. Specifically, Th<sub>1</sub> cells upregulate antigen presentation and as such regulate the duration and magnitude of CD8<sup>+</sup> T-cell response, whereas Tregs increase immunosuppressive cytokines and inhibit CD8<sup>+</sup> T-cell function.<sup>52</sup> Thus immunodepleting all CD4<sup>+</sup> may not reveal the role of these distinct populations. We further appreciate that even CD8<sup>+</sup> T cells present with varying phenotypes, which we have not addressed here and requires further studies.



In summary, our data are the first to describe an increase in renal T cells associated with disease severity, a specific activation of CD8<sup>+</sup> T cells, and a functional role of these cells in inhibiting cystogenesis. Hence, we suggest that immunotherapies leading to reactivation of T cells may represent a novel therapeutic strategy. Because such agents, including immune checkpoint inhibitors, are FDA approved for multiple cancers and specifically act on CD8<sup>+</sup> T-cell reactivation, it raises the possibility of repurposing these drugs for use in people with ADPKD.

## CONCISE METHODS

Full methods are available in the Supplementary Methods.

### Mouse models

We used the C57Bl/6, 129/S6, and Balb/c *Pkd1*<sup>RC/RC</sup> model and the C57Bl/6 *Pkd1*<sup>RC/-</sup> model, as previously published.<sup>55,71</sup> WT control subjects were obtained from Jackson Laboratory, Bar Harbor, ME or Taconic Biosciences Inc, Rensselaer, NY.

### Human samples

De-identified human ADPKD/ARPKD and normal human kidney formalin-fixed, paraffin-embedded sections were obtained from the Kansas PKD Research and Translational Core Center (P30 DK106912) at the University of Kansas Medical Center.

### Kidney function analyses

Blood urea nitrogen was measured using the QuantiChrom Urea Assay Kit (BioAssay Systems, Hayward, CA) according to the manufacturer's protocol. Plasma creatinine concentration was analyzed with high-performance liquid chromatography-tandem-mass spectrometry (HPLC-MS/MS; Applied Biosystems 3200 Q TRAP, Foster City, CA).<sup>83</sup>

### Histomorphometric analysis

Cystic index, cyst size, and cyst number were analyzed using a custom-built NIS-Elements AR v4.6 macro (Nikon, Minato, Tokyo, Japan). Fibrotic area was analyzed from picosirius red-stained kidney sections, visualized using an Olympus BX41 microscope (Olympus Corporation, Center Valley, PA) with a linear polarizer.

### Cell culture

All cell lines have been previously described.<sup>64,84</sup> Cells were grown in either DMEM/F12 +L-glutamine, 15nM HEPES (Corning Inc., Corning, NY; RCTE, 9-12) or RPMI-1640 +L-glutamine (Corning; HCC827) supplemented with 10% fetal bovine serum (VWR International, Radnor, PA) and 1% penicillin-streptomycin (Corning).

### Proliferation assay

RCTE and 9-12 cells were treated for 72 hours with IFN- $\gamma$  (100 ng/ml) or phosphate-buffered saline solution (control) and subsequently counted using the Cellometer Auto T4 (Nexcelom Bioscience, Lawrence, MA).

## Immunofluorescence Labeling/Quantification

Tissues were prepared for IF labeling as previously described<sup>55</sup> with the following modification: Autofluorescence quenching with 0.1% Sudan Black in 70% ethanol, 2-hour antigen retrieval at 100 °C, washes in tris-buffered saline solution and Tween 20 (TBST). Terminal deoxynucleotidyltransferase-mediated dUTP nick end-labeling staining was performed according to the manufacturer's protocol (*In Situ* Cell Death Detection Kit, TMR red; Sigma-Aldrich Inc., St. Louis, MO). Quantification was performed using NIS-Elements AR v4.6 (Nikon). Antibody details can be found in the Supplementary Methods.

## Quantitative polymerase chain reaction

Renal tissue RNA was isolated from a small piece of flash-frozen tissue using the RNeasy Plus Mini Kit (Qiagen, Germantown, MD) and cDNA was synthesized using the qScript XLT cDNA SuperMix (Quantabio, Beverly, MA). For human cell RNA, RCTE, 9–12, and HCC827 cells were treated with IFN- $\gamma$  (100 ng/ml) or phosphate-buffered saline solution (control) for 24 hours prior to RNA isolation. Quantitative polymerase chain reaction was performed using the PowerSYBER PCR Master Mix (Applied Biosystems) on a CFX96 Real-Time System (Bio-Rad Laboratories, Hercules, CA). Primer details can be found in the Supplementary Methods.

## Single cell suspension

Dissected kidney and spleen tissue were mechanically dissociated and digested in a mixture containing DMEM/F12, Liberase TL, and DNaseI at 37 °C for 30 minutes. Dissociation was completed using an 18G needle and quenched using FA3 buffer. Cells were passed through a 100  $\mu$ m filter, underwent a red blood cell lysis, and then were passed through a 70- $\mu$ m filter.

## Flow cytometry

**T-cell panel protocol.**—The single cell suspension was blocked in anti-mouse CD16/CD32 on a rocker for 15 minutes at 4 °C. Fix viability dye and conjugated antibodies were then added, and cells were incubated in the dark on a rocker at 4 °C for 45 minutes. Cells were resuspended in FA3 buffer and ran on the Gallios Flow Cytometer Machine (Beckman Coulter, Brea, CA). Antibody details can be found in the Supplementary Methods.

**Confirmation of CD8<sup>+</sup> T-cell depletion (collection/flow protocol).**—Whole blood (50  $\mu$ l) from a submandibular blood draw was collected in 10  $\mu$ l heparin. Blood was lysed in 3 ml of red blood cell lysis buffer for 3 minutes at room temperature, quenched with FA3 buffer, and pelleted. Pellets were stained/analyzed as previously described.

**Data analysis.**—Data were analyzed using the Kaluza Analysis v1.5 software (Beckman Coulter). A gating workflow is shown in Supplementary Figure 7A.

## CD8<sup>+</sup> T-cell depletion

One-month-old C57Bl/6 or 129/S6 *Pkd1*<sup>RC/RC</sup> mice were treated twice a week for 8 weeks by i.p. injection with 10 mg/kg anti-CD8<sup>+</sup> depleting antibody or 10 mg/kg IgG2a control

(BioXCell, West Lebanon, NH). After 8 weeks of treatment, the animals were killed and evaluated as previously described.

### ***In situ* hybridization**

*In situ* hybridization was performed using the RNAscope RED assay kit (ACDBio, Newark, CA) combined with immunofluorescence. Probe information can be found in the Supplementary Methods.

### **Statistical analysis**

All analyses were performed using PRISM7 (GraphPad Software, La Jolla, CA). Data were analyzed by a nonparametric Mann-Whitney test to determine statistical significance unless otherwise noted and presented as the mean and standard error of the mean (SEM). *P* values are denoted by \*(*P* 0.05), \*\*(*P* 0.01), \*\*\*(*P* 0.001), and \*\*\*\*(*P* 0.0001).

### **Supplementary Material**

Refer to Web version on PubMed Central for supplementary material.

### **ACKNOWLEDGMENTS**

The work was partially supported by a Pilot & Feasibility Grant from the Consortium for Fibrosis Research and Translation, University of Colorado Anschutz Medical Campus, Aurora, Colorado, USA. EK and LT were supported by a T32 (NIDDK 5T32DK007135 [EK], NIGMS 5T32GM007635 [LT]). The *Pkd1*<sup>RC/RC</sup> mouse model was graciously provided by the Mayo Clinic Robert M. and Billie Kelley Pirnie Translational Polycystic Kidney Disease Research Center (NIDDK P30 DK090728). ADPKD/ARPKD and normal human kidney tissues were provided by the PKD Biomarkers and Biomaterials Core in the Kansas PKD Research and Translational Core Center (P30 DK106912) at the University of Kansas Medical Center. Human tissues were obtained with the assistance of the KU Cancer Center's Biospecimen Repository (P30 CA168524) and hospitals participating in the PKD Foundation's tissue donation program. George S. DeBeck (Nikon Instruments Inc.) aided in the development of the histomorphometric analysis macro for the cystic kidney.

### **REFERENCES**

1. Grantham JJ. Mechanisms of progression in autosomal dominant polycystic kidney disease. *Kidney Int Suppl.* 1997;63:S93–S97. [PubMed: 9407432]
2. Grantham JJ, Chapman AB, Torres VE. Volume progression in autosomal dominant polycystic kidney disease: the major factor determining clinical outcomes. *Clin J Am Soc Nephrol.* 2006;1:148–157. [PubMed: 17699202]
3. Heyer CM, Sundsbak JL, Abebe KZ, et al. Predicted mutation strength of nontruncating PKD1 mutations aids genotype-phenotype correlations in autosomal dominant polycystic kidney disease. *J Am Soc Nephrol.* 2016;27:2872–2884. [PubMed: 26823553]
4. Porath B, Gainullin VG, Cornec-Le Gall E, et al. Mutations in GANAB, encoding the glucosidase IIalpha subunit, cause autosomal-dominant polycystic kidney and liver disease. *Am J Hum Genet.* 2016;98:1193–1207. [PubMed: 27259053]
5. Grantham JJ. Clinical practice. Autosomal dominant polycystic kidney disease. *N Engl J Med.* 2008;359:1477–1485. [PubMed: 18832246]
6. Iglesias CG, Torres VE, Offord KP, et al. Epidemiology of adult polycystic kidney disease, Olmsted County, Minnesota: 1935-1980. *Am J Kidney Dis.* 1983;2:630–639. [PubMed: 6846334]
7. Peters DJ, Sandkuijl LA. Genetic heterogeneity of polycystic kidney disease in Europe. *Contrib Nephrol.* 1992;97:128–139. [PubMed: 1633713]
8. Torres VE, Harris PC, Pirson Y. Autosomal dominant polycystic kidney disease. *Lancet.* 2007;369:1287–1301. [PubMed: 17434405]

9. Grantham JJ, Torres VE, Chapman AB, et al. Volume progression in polycystic kidney disease. *N Engl J Med.* 2006;354:2122–2130. [PubMed: 16707749]
10. Rahman E, Niaz FA, Al-Suwaida A, et al. Analysis of causes of mortality in patients with autosomal dominant polycystic kidney disease: a single center study. *Saudi J Kidney Dis Transpl.* 2009;20:806–810. [PubMed: 19736478]
11. Perrone RD, Ruthazer R, Terrin NC. Survival after end-stage renal disease in autosomal dominant polycystic kidney disease: contribution of extrarenal complications to mortality. *Am J Kidney Dis.* 2001;38:777–784. [PubMed: 11576881]
12. Harris PC, Torres VE. Genetic mechanisms and signaling pathways in autosomal dominant polycystic kidney disease. *J Clin Invest.* 2014;124:2315–2324. [PubMed: 24892705]
13. Walz G, Budde K, Manna M, et al. Everolimus in patients with autosomal dominant polycystic kidney disease. *N Engl J Med.* 2010;363:830–840. [PubMed: 20581392]
14. Serra AL, Poster D, Kistler AD, et al. Sirolimus and kidney growth in autosomal dominant polycystic kidney disease. *N Engl J Med.* 2010;363:820–829. [PubMed: 20581391]
15. Torres VE, Chapman AB, Devuyst O, et al. Tolvaptan in patients with autosomal dominant polycystic kidney disease. *N Engl J Med.* 2012;367:2407–2418. [PubMed: 23121377]
16. Caroli A, Perico N, Perna A, et al. Effect of longacting somatostatin analogue on kidney and cyst growth in autosomal dominant polycystic kidney disease (ALADIN): a randomised, placebo-controlled, multicenter trial. *Lancet.* 2013;382:1485–1495. [PubMed: 23972263]
17. Irazabal MV, Torres VE. Experimental therapies and ongoing clinical trials to slow down progression of ADPKD. *Curr Hypertens Rev.* 2013;9:44–59. [PubMed: 23971644]
18. Harris PC, Torres VE. Polycystic kidney disease, autosomal dominant. *GeneReviews.* Available at: <https://www.ncbi.nlm.nih.gov/books/NBK1246/>. Published January 10, 2002; updated July 19, 2018 Accessed July 20, 2018.
19. Mochizuki T, Wu G, Hayashi T, et al. PKD2, a gene for polycystic kidney disease that encodes an integral membrane protein. *Science.* 1996;272:1339–1342. [PubMed: 8650545]
20. The polycystic kidney disease 1 gene encodes a 14 kb transcript and lies within a duplicated region on chromosome 16. The European Polycystic Kidney Disease Consortium. *Cell.* 1994;77:881–894. [PubMed: 8004675]
21. Zerres K, Rudnik-Schoneborn S, Deget F. Childhood onset autosomal dominant polycystic kidney disease in sibs: clinical picture and recurrence risk. German Working Group on Paediatric Nephrology (Arbeitsgemeinschaft fuer Padiatrische Nephrologie). *J Med Genet.* 1993;30:583–588. [PubMed: 8411032]
22. Bergmann C, Bruchle NO, Frank V, et al. Perinatal deaths in a family with autosomal dominant polycystic kidney disease and a PKD2 mutation. *N Engl J Med.* 2008;359:318–319. [PubMed: 18635443]
23. Hateboer N, v Dijk MA, Bogdanova N, et al. Comparison of phenotypes of polycystic kidney disease types 1 and 2. European PKD1-PKD2 Study Group. *Lancet.* 1999;353:103–107. [PubMed: 10023895]
24. Harris PC, Rossetti S. Determinants of renal disease variability in ADPKD. *Adv Chronic Kidney Dis.* 2010;17:131–139. [PubMed: 20219616]
25. Torres VE, Harris PC. Autosomal dominant polycystic kidney disease: the last 3 years. *Kidney Int.* 2009;76:149–168. [PubMed: 19455193]
26. Nauli SM, Alenghat FJ, Luo Y, et al. Polycystins 1 and 2 mediate mechanosensation in the primary cilium of kidney cells. *Nat Genet.* 2003;33:129–137. [PubMed: 12514735]
27. Delling M, Indzhykulian AA, Liu X, et al. Primary cilia are not calcium-responsive mechanosensors. *Nature.* 2016;531:656–660. [PubMed: 27007841]
28. Delling M, DeCaen PG, Doerner JF, et al. Primary cilia are specialized calcium signalling organelles. *Nature.* 2013;504:311–314. [PubMed: 24336288]
29. Grantham JJ. Polycystic kidney disease: neoplasia in disguise. *Am J Kidney Dis.* 1990;15:110–116. [PubMed: 2405652]
30. Seeger-Nukpezah T, Geynisman DM, Nikonova AS, et al. The hallmarks of cancer: relevance to the pathogenesis of polycystic kidney disease. *Nat Rev Nephrol.* 2015;11:515–534. [PubMed: 25870008]

31. Hanahan D, Weinberg RA. Hallmarks of cancer: the next generation. *Cell*. 2011;144:646–674. [PubMed: 21376230]
32. Nadasdy T, Laszik Z, Lajoie G, et al. Proliferative activity of cyst epithelium in human renal cystic diseases. *J Am Soc Nephrol*. 1995;5:1462–1468. [PubMed: 7703384]
33. Battini L, Macip S, Fedorova E, et al. Loss of polycystin-1 causes centrosome amplification and genomic instability. *Hum Mol Genet*. 2008;17:2819–2833. [PubMed: 18566106]
34. Li M, Qin S, Wang L, et al. Genomic instability in patients with autosomal-dominant polycystic kidney disease. *J Int Med Res*. 2013;41:169–175. [PubMed: 23569143]
35. Brasier JL, Henske EP. Loss of the polycystic kidney disease (PKD1) region of chromosome 16p13 in renal cyst cells supports a loss-of-function model for cyst pathogenesis. *J Clin Invest*. 1997;99:194–199. [PubMed: 9005987]
36. Rowe I, Chiaravalli M, Mannella V, et al. Defective glucose metabolism in polycystic kidney disease identifies a new therapeutic strategy. *Nat Med*. 2013;19:488–493. [PubMed: 23524344]
37. Warner G, Hein KZ, Nin V, et al. Food restriction ameliorates the development of polycystic kidney disease. *J Am Soc Nephrol*. 2016;27:1437–1447. [PubMed: 26538633]
38. Zheng D, Wolfe M, Cowley BD, Jr., et al. Urinary excretion of monocyte chemoattractant protein-1 in autosomal dominant polycystic kidney disease. *J Am Soc Nephrol*. 2003;14:2588–2595. [PubMed: 14514736]
39. Li X, Magenheimer BS, Xia S, et al. A tumor necrosis factor- $\alpha$ -mediated pathway promoting autosomal dominant polycystic kidney disease. *Nat Med*. 2008;14:863–868. [PubMed: 18552856]
40. Ta MH, Harris DC, Rangan GK. Role of interstitial inflammation in the pathogenesis of polycystic kidney disease. *Nephrology (Carlton)*. 2013;18:317–330. [PubMed: 23448509]
41. Karihaloo A, Koraihy F, Huen SC, et al. Macrophages promote cyst growth in polycystic kidney disease. *J Am Soc Nephrol*. 2011;22:1809–1814. [PubMed: 21921140]
42. Swenson-Fields KI, Vivian CJ, Salah SM, et al. Macrophages promote polycystic kidney disease progression. *Kidney Int*. 2013;83:855–864. [PubMed: 23423256]
43. Vogler C, Homan S, Pung A, et al. Clinical and pathologic findings in two new allelic murine models of polycystic kidney disease. *J Am Soc Nephrol*. 1999;10:2534–2539. [PubMed: 10589692]
44. Zeier M, Fehrenbach P, Geberth S, et al. Renal histology in polycystic kidney disease with incipient and advanced renal failure. *Kidney Int*. 1992;42:1259–1265. [PubMed: 1453612]
45. McPherson EA, Luo Z, Brown RA, et al. Chymase-like angiotensin II-generating activity in end-stage human autosomal dominant polycystic kidney disease. *J Am Soc Nephrol*. 2004;15:493–500. [PubMed: 14747398]
46. Bernhardt WM, Wiesener MS, Weidemann A, et al. Involvement of hypoxia-inducible transcription factors in polycystic kidney disease. *Am J Pathol*. 2007;170:830–842. [PubMed: 17322369]
47. Werder AA, Amos MA, Nielsen AH, et al. Comparative effects of germfree and ambient environments on the development of cystic kidney disease in CFWwd mice. *J Lab Clin Med*. 1984;103:399–407. [PubMed: 6699465]
48. Locatelli L, Cadamuro M, Spirli C, et al. Macrophage recruitment by fibrocystin-defective biliary epithelial cells promotes portal fibrosis in congenital hepatic fibrosis. *Hepatology*. 2016;63:965–982. [PubMed: 26645994]
49. Callahan MK, Wolchok JD. At the bedside: CTLA-4- and PD-1-blocking antibodies in cancer immunotherapy. *J Leukoc Biol*. 2013;94:41–53. [PubMed: 23667165]
50. Topalian SL, Drake CG, Pardoll DM. Immune checkpoint blockade: a common denominator approach to cancer therapy. *Cancer Cell*. 2015;27:450–461. [PubMed: 25858804]
51. Restifo NP, Dudley ME, Rosenberg SA. Adoptive immunotherapy for cancer: harnessing the T cell response. *Nat Rev Immunol*. 2012;12:269–281. [PubMed: 22437939]
52. DeNardo DG, Andreu P, Coussens LM. Interactions between lymphocytes and myeloid cells regulate pro- versus anti-tumor immunity. *Cancer Metastasis Rev*. 2010;29:309–316. [PubMed: 20405169]
53. Ribas A, Hamid O, Daud A, et al. Association of pembrolizumab with tumor response and survival among patients with advanced melanoma. *JAMA*. 2016;315:1600–1609. [PubMed: 27092830]

54. Long GV, Weber JS, Larkin J, et al. Nivolumab for patients with advanced melanoma treated beyond progression: analysis of 2 phase 3 clinical trials. *JAMA Oncol.* 2017;3:1511–1519. [PubMed: 28662232]
55. Hopp K, Ward CJ, Hommerding CJ, et al. Functional polycystin-1 dosage governs autosomal dominant polycystic kidney disease severity. *J Clin Invest.* 2012;122:4257–4273. [PubMed: 23064367]
56. Rossetti S, Kubly VJ, Consugar MB, et al. Incompletely penetrant PKD1 alleles suggest a role for gene dosage in cyst initiation in polycystic kidney disease. *Kidney Int.* 2009;75:848–855. [PubMed: 19165178]
57. Nakajima C, Uekusa Y, Iwasaki M, et al. A role of interferon-gamma (IFN-gamma) in tumor immunity: T cells with the capacity to reject tumor cells are generated but fail to migrate to tumor sites in IFN-gamma-deficient mice. *Cancer Res.* 2001;61:3399–3405. [PubMed: 11309299]
58. Marshall A, Celentano A, Cirillo N, et al. Tissue-specific regulation of CXCL9/10/11 chemokines in keratinocytes: implications for oral inflammatory disease. *PLoS One.* 2017;12:e0172821. [PubMed: 28253295]
59. Lucca LE, Hafler DA. Resisting fatal attraction: a glioma oncometabolite prevents CD8+ T cell recruitment. *J Clin Invest.* 2017;127:1218–1220. [PubMed: 28319049]
60. Tokunaga R, Zhang W, Naseem M, et al. CXCL9, CXCL10, CXCL11/CXCR3 axis for immune activation—a target for novel cancer therapy. *Cancer Treat Rev.* 2017;63:40–47. [PubMed: 29207310]
61. Bronger H, Singer J, Windmuller C, et al. CXCL9 and CXCL10 predict survival and are regulated by cyclooxygenase inhibition in advanced serous ovarian cancer. *Br J Cancer.* 2016;115:553–563. [PubMed: 27490802]
62. Kistner L, Doll D, Holtorf A, et al. Interferon-inducible CXC-chemokines are crucial immune modulators and survival predictors in colorectal cancer. *Oncotarget.* 2017;8:89998–90012. [PubMed: 29163806]
63. Ding Q, Lu P, Xia Y, et al. CXCL9: evidence and contradictions for its role in tumor progression. *Cancer Med.* 2016;5:3246–3259. [PubMed: 27726306]
64. Loghman-Adham M, Nauli SM, Soto CE, et al. Immortalized epithelial cells from human autosomal dominant polycystic kidney cysts. *Am J Physiol Renal Physiol.* 2003;285:F397–F412. [PubMed: 12734101]
65. Buszello H Antiproliferative effects of four different cytokines on renal carcinoma cell lines. *Anticancer Res.* 1995;15:735–738. [PubMed: 7645950]
66. Bromberg JF, Horvath CM, Wen Z, et al. Transcriptionally active Stat1 is required for the antiproliferative effects of both interferon alpha and interferon gamma. *Proc Natl Acad Sci U S A.* 1996;93:7673–7678. [PubMed: 8755534]
67. Fazekas de St Groth B, Smith AL, Higgins CA. T cell activation: in vivo veritas. *Immunol Cell Biol.* 2004;82:260–268. [PubMed: 15186257]
68. Borrego F, Robertson MJ, Ritz J, et al. CD69 is a stimulatory receptor for natural killer cell and its cytotoxic effect is blocked by CD94 inhibitory receptor. *Immunology.* 1999;97:159–165. [PubMed: 10447727]
69. Huang XR, Tipping PG, Shuo L, et al. Th1 responsiveness to nephritogenic antigens determines susceptibility to crescentic glomerulonephritis in mice. *Kidney Int.* 1997;51:94–103. [PubMed: 8995722]
70. Sadick MD, Heinzl FP, Shigekane VM, et al. Cellular and humoral immunity to *Leishmania major* in genetically susceptible mice after in vivo depletion of L3T4+ T cells. *J Immunol.* 1987;139:1303–1309. [PubMed: 3112230]
71. Muto S, Aiba A, Saito Y, et al. Pioglitazone improves the phenotype and molecular defects of a targeted Pkd1 mutant. *Hum Mol Genet.* 2002;11:1731–1742. [PubMed: 12095915]
72. Klawitter J, Klawitter J, McFann K, et al. Bioactive lipid mediators in polycystic kidney disease. *J Lipid Res.* 2014;55:1139–1149. [PubMed: 24343898]
73. Menon V, Rudym D, Chandra P, et al. Inflammation, oxidative stress, and insulin resistance in polycystic kidney disease. *Clin J Am Soc Nephrol.* 2011;6:7–13. [PubMed: 20829421]



74. Mrug M, Zhou J, Guay-Woodford LM, et al. Renal macrophages in autosomal recessive polycystic kidney disease. *Nephrology (Carlton)*. 2013;18:746. [PubMed: 24571748]
75. Schreiber RD, Old LJ, Smyth MJ. Cancer immunoediting: integrating immunity's roles in cancer suppression and promotion. *Science*. 2011;331:1565–1570. [PubMed: 21436444]
76. Gong J, Chehrazhi-Raffle A, Reddi S, et al. Development of PD-1 and PD-L1 inhibitors as a form of cancer immunotherapy: a comprehensive review of registration trials and future considerations. *J Immunother Cancer*. 2018;6:8. [PubMed: 29357948]
77. Wilson RAM, Evans TRJ, Fraser AR, et al. Immune checkpoint inhibitors: new strategies to checkmate cancer. *Clin Exp Immunol*. 2018;191:133–148. [PubMed: 29139554]
78. Spranger S, Sivan A, Corrales L, et al. Tumor and host factors controlling antitumor immunity and efficacy of cancer immunotherapy. *Adv Immunol*. 2016;130:75–93. [PubMed: 26923000]
79. Pardoll DM. The blockade of immune checkpoints in cancer immunotherapy. *Nat Rev Cancer*. 2012;12:252–264. [PubMed: 22437870]
80. Wanchoo R, Karam S, Uppal NN, et al. Adverse renal effects of immune checkpoint inhibitors: a narrative review. *Am J Nephrol*. 2017;45:160–169. [PubMed: 28076863]
81. Martini DJ, Hamieh L, McKay RR, et al. Durable Clinical benefit in metastatic renal cell carcinoma patients who discontinue PD-1/PD-L1 therapy for immune-related adverse events. *Cancer Immunol Res*. 2018;6:402–408. [PubMed: 29437040]
82. Lipson EJ, Sharfman WH, Drake CG, et al. Durable cancer regression off-treatment and effective reinduction therapy with an anti-PD-1 antibody. *Clin Cancer Res*. 2013;19:462–468. [PubMed: 23169436]
83. Masuda M, Miyazaki-Anzai S, Keenan AL, et al. Activating transcription factor-4 promotes mineralization in vascular smooth muscle cells. *JCI Insight*. 2016;1:e88646. [PubMed: 27812542]
84. Coldren CD, Helfrich BA, Witta SE, et al. Baseline gene expression predicts sensitivity to gefitinib in non-small cell lung cancer cell lines. *Mol Cancer Res*. 2006;4:521–528. [PubMed: 16877703]

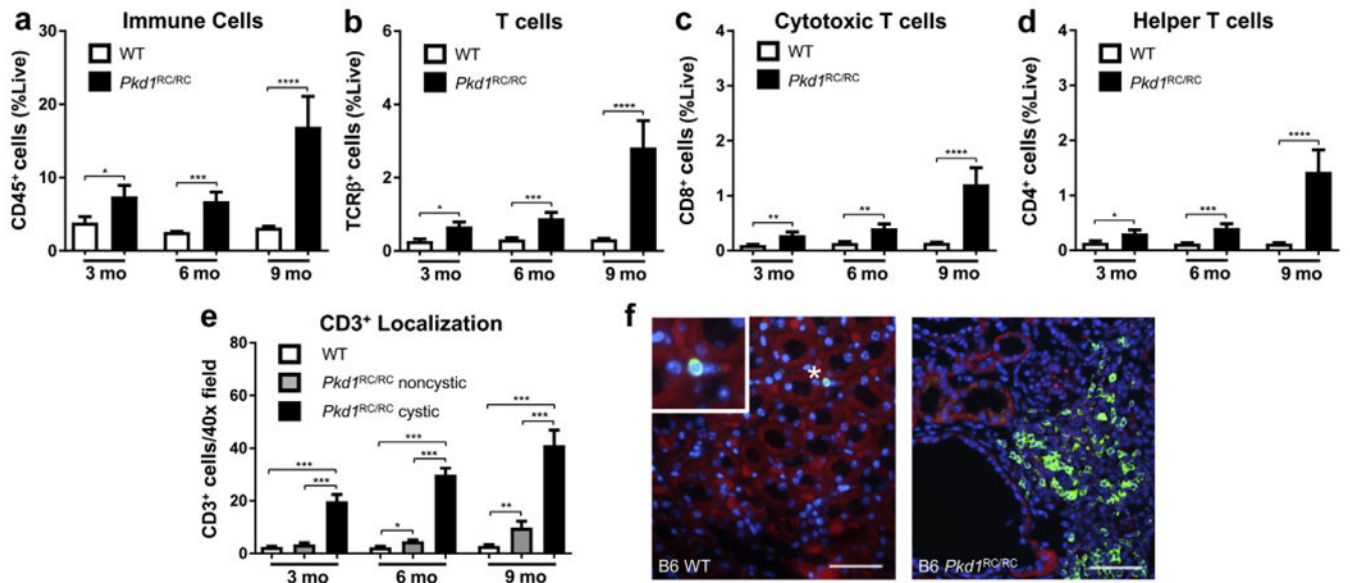


**Figure 1. Autosomal dominant polycystic kidney disease (ADPKD) pathology triggers an increase of the adaptive immune system in the C57Bl/6 *Pkd1<sup>RC/RC</sup>* model.**

Wild type (WT) and *Pkd1<sup>RC/RC</sup>* C57Bl/6 mice were aged to 3, 6, and 9 months and flow cytometry of a renal single cell suspension was used to assess differences in the adaptive immune system at varying disease stages. An increase in immune cells (CD45<sup>+</sup>) (a), T cells (T-cell receptor  $\beta^+$  [TCR $\beta^+$ ]) (b), cytotoxic T cells (CD8<sup>+</sup>) (c), and helper T cells (CD4<sup>+</sup>) (d) was observed in *Pkd1<sup>RC/RC</sup>* mice compared with WT control subjects across all 3 time points, but the increase was most striking at 9 months. Immunofluorescence (IF) imaging of formalin-fixed paraffin embedded tissue showed specific localization of T cells (CD3<sup>+</sup>, comparable marker to TCR $\beta$ ) near cystic lesions rather than normal tissue even at early disease stages where the overall increase in T-cell numbers was modest (e). (f)

Representative IF images showing CD3<sup>+</sup> localization near cystic epithelium in a 6-month-old C57Bl/6 *Pkd1<sup>RC/RC</sup>* mouse (4',6-diamidino-2-phenylindole [DAPI] = blue; CD3 = green; E-cadherin = red; bar = 50  $\mu$ m). Data are represented as mean  $\pm$  SEM, and a nonparametric Mann-Whitney test was performed on the data. \**P* 0.05; \*\**P* 0.01; \*\*\**P* 0.001; \*\*\*\**P* 0.0001. *N* = 10 mice per group (5 females, 5 males). To optimize viewing of this image, please see the online version of this article at [www.kidney-international.org](http://www.kidney-international.org).

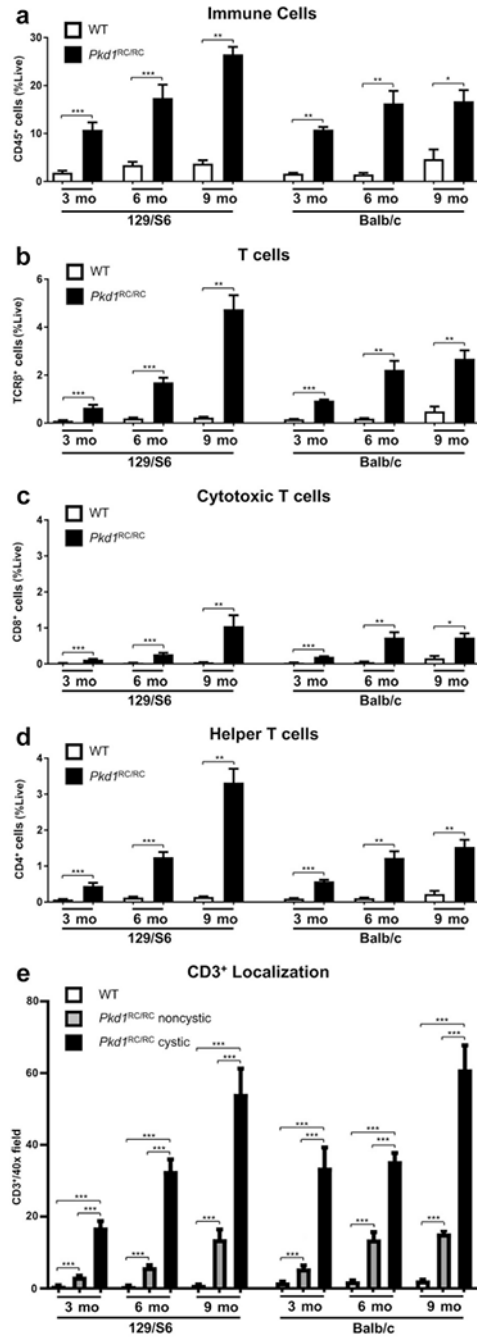


**Figure 2. The increase of renal adaptive immune cells is augmented in strains with more severe autosomal dominant polycystic kidney disease (ADPKD).** Renal single cell suspensions of wild type (WT) and *Pkd1<sup>RC/RC</sup>* 129/S6 and Balb/c mice were analyzed in the same manner as for the C57Bl/6 strain. A more rapid increase, notably at younger ages, of CD45<sup>+</sup> (a), T-cell receptor β<sup>+</sup> (TCRR<sup>+</sup>) (b), CD8<sup>+</sup> (c), and CD4<sup>+</sup> (d) cells was observed in the *Pkd1<sup>RC/RC</sup>* compared with WT mice of these strains with more rapidly progressive disease. Immunofluorescence quantification of CD3<sup>+</sup> T cells shows a larger number of positive cells near cystic lesions from a very young age on and only a

modest increase over time, correlating with the high cystic burden these animals present with at 3 months (e). Data are represented as mean  $\pm$  SEM, and a nonparametric Mann-Whitney test was performed on the data. \* $P$  0.05; \*\* $P$  0.01; \*\*\* $P$  0.001.  $N$  6 mice per group (one-half females, one-half males).

Author Manuscript

Author Manuscript

Author Manuscript

Author Manuscript

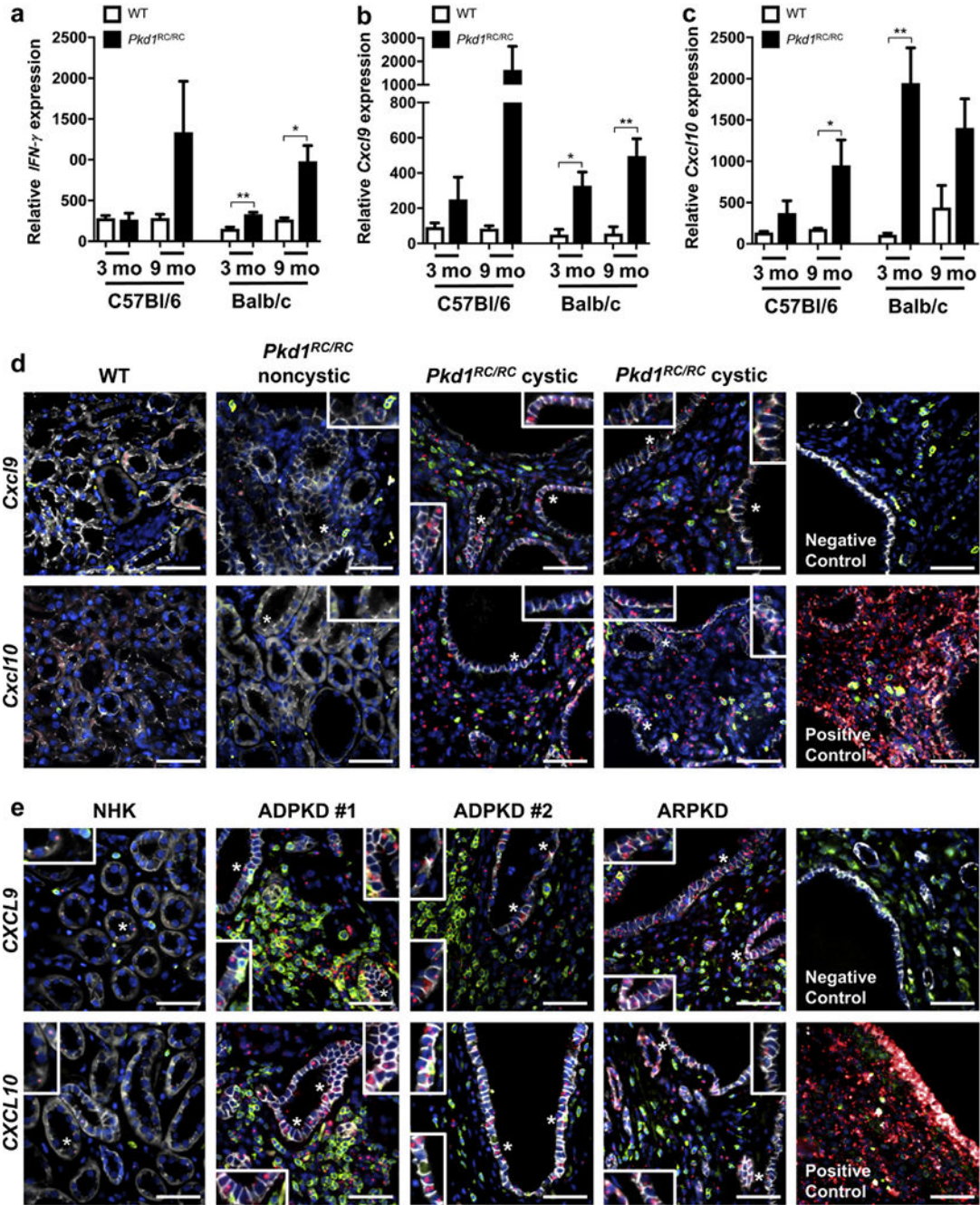


**Figure 3. T-cell recruiting chemokines and T-cell secreted cytokines are increased in autosomal dominant polycystic kidney disease (ADPKD).**

Quantitative polymerase chain reaction (qPCR) of RNA isolated from whole kidney pieces of wild type (WT) and *Pkd1<sup>RC/RC</sup>* mice showed increased levels of interferon (IFN)- $\gamma$ , a cytokine secreted by CD8<sup>+</sup> T cells (a) and chemokines known to recruit T cells (b, *Cxcl9* and c, *Cxcl10*) when comparing *Pkd1<sup>RC/RC</sup>* with WT mice in both the mild C57Bl/6 and the severe Balb/c background (relative cytokine/chemokine levels may not correlate to disease severity because RNA was isolated from only a small kidney piece, ignoring the

nonhomogeneous nature of the disease). **(d)** Representative *in situ* hybridization images of 3-month-old Balb/c mice. In WT mice, staining for *Cxcl9/Cxcl10* (red) with immunofluorescent co-staining for CD3 (green) and E-cadherin (white) showed no *Cxcl9/Cxcl10* expression in microenvironmental cells or renal tubules; 4',6-diamidino-2-phenylindole [DAPI] = blue. Little *Cxcl9/Cxcl10* was detected in noncystic regions of *Pkd1<sup>RC/RC</sup>* mice; however, much higher levels of the chemokines were observed in cystic regions where significant numbers of T cells accumulate. Interestingly, both chemokines were also produced by the cystic epithelium and not only by cells within the cystic microenvironment (insets). **(e)** T-cell infiltration to cystic regions and *CXCL9/CXCL10* production by microenvironmental cells and tubular epithelium (insets) were confirmed in human formalin-fixed, paraffin-embedded (FFPE) tissue. Very few T cells (CD3 = green) were infiltrating normal human kidneys (NHKs), and only low levels of *CXCL9/CXCL10* (*in situ* = red) could be detected within the microenvironment or epithelium (E-cadherin = white; 4',6-diamidino-2-phenylindole [DAPI] = blue). As for *Pkd1<sup>RC/RC</sup>* mice, the number of renal T cells were significantly increased in ADPKD/ARPKD patient tissue versus NHK and located predominantly to cystic regions. Here also, significant levels of both chemokines could be detected in the microenvironment and tubular epithelium. Staining of positive and negative control probes for *in situ* staining are shown. Data are represented as mean  $\pm$  SEM, and a nonparametric Mann-Whitney test was performed on the data. \**P* 0.05; \*\**P* 0.01. *N* = 6 mice per group (one-half females, one-half males). Bar = 50  $\mu$ m. ARPKD, autosomal recessive polycystic kidney disease. To optimize viewing of this image, please see the online version of this article at [www.kidney-international.org](http://www.kidney-international.org).



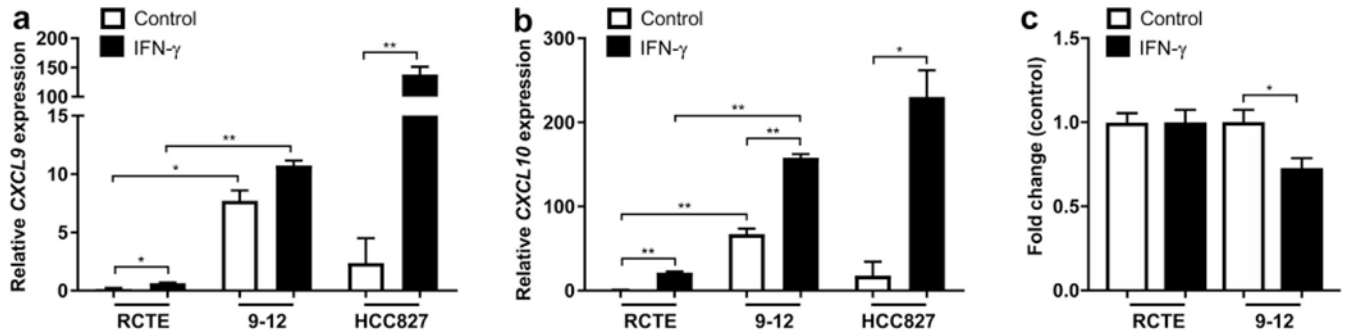


**Figure 4. Interferon (IFN)- $\gamma$  stimulates chemokine production and inhibits cell proliferation in autosomal dominant polycystic kidney disease (ADPKD) epithelial cells.**

IFN- $\gamma$  treatment for 24 hours of renal cortical tubular epithelial (RCTE) ( $PKD1^{+/+}$ ) and 9-12 ( $PKD1^{-/-}$ ) epithelial cells stimulated expression of *CXCL9* (a) and *CXCL10* (b) mRNA as shown *in vivo* in  $Pkd1^{RC/RC}$  mice, confirming the ability of tubular epithelia to produce these chemokines. Interestingly, 9-12 cells produced significantly higher basal levels of the chemokines compared with RCTE control cells. The lung adenocarcinoma cell line HCC827 was used as a positive control for the induction of *CXCL9/CXCL10* after IFN- $\gamma$  stimulation. (c) RCTE ( $PKD1^{+/+}$ ) and 9-12 ( $PKD1^{-/-}$ ) cells were treated with IFN- $\gamma$  for 72 hours followed by assessment of cell count. The 9-12 cells treated with IFN- $\gamma$  had a lower cell count compared with RCTE cells, consistent with an antiproliferative role of IFN- $\gamma$ . The cell count was normalized to control-treated. Data are represented as mean  $\pm$  SEM, and a unpaired *t*-test was performed on the data. \* $P$  0.05; \*\* $P$  0.01.

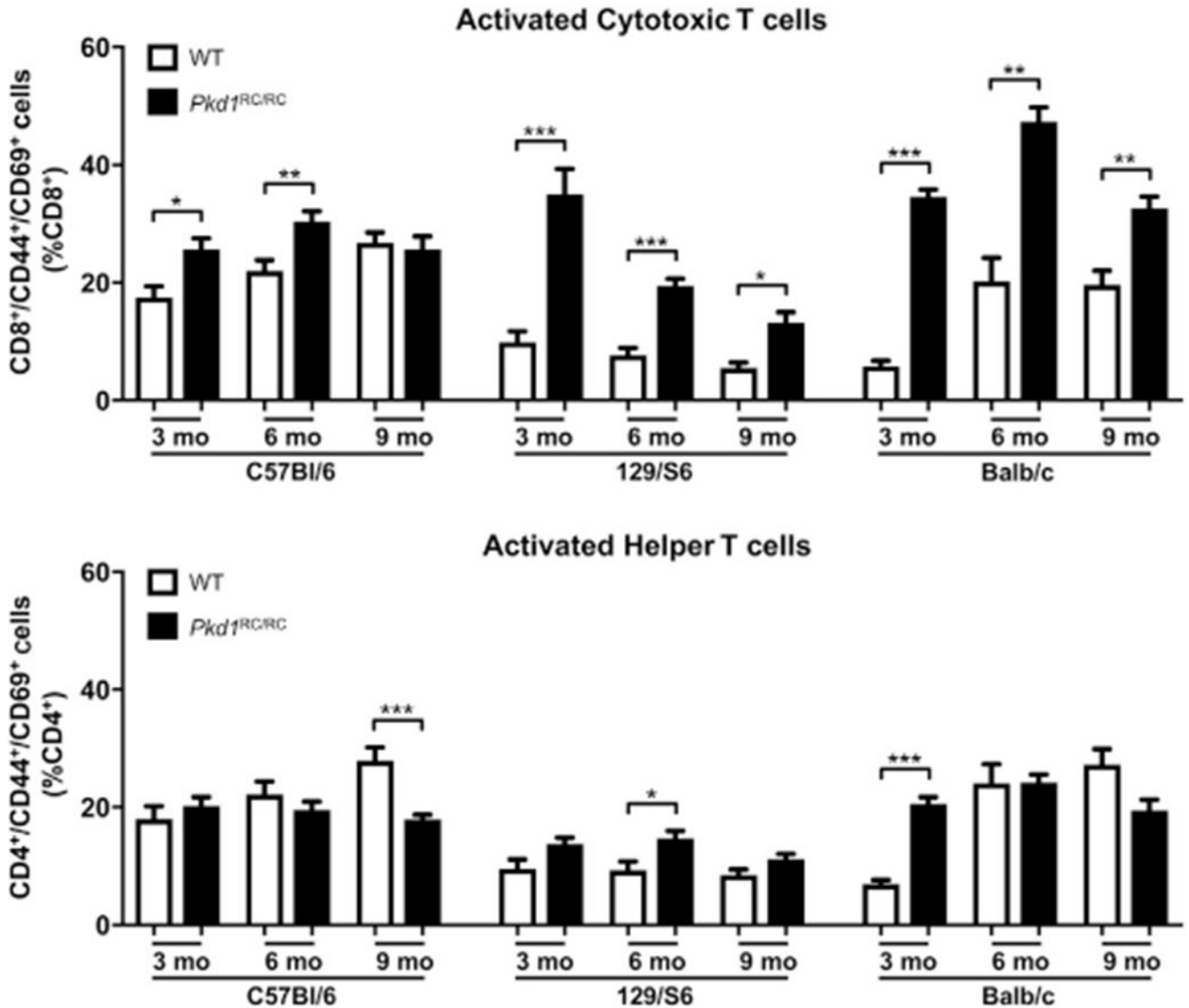


**Figure 5. CD8<sup>+</sup> T cells are predominantly activated in the *Pkd1*<sup>RC/RC</sup> mouse model of autosomal dominant polycystic kidney disease (ADPKD).**

Wild type (WT) and *Pkd1*<sup>RC/RC</sup> mice were aged to 3,6, and 9 months and flow cytometry of a renal single cell suspension was used to assess differences in activation of CD8<sup>+</sup> and CD4<sup>+</sup> T cells at varying disease stages. In all 3 strains, CD8<sup>+</sup> T cells were preferentially activated based on the T-cell activation markers CD44/CD69 at early disease stages. Comparably, CD4<sup>+</sup> T cells did not show an increase in activation relative to WT at any disease stage. Importantly, CD8<sup>+</sup> T cells were significantly more activated in 129/S6 and Balb/c ADPKD mice, correlative with their higher disease burden. Data are represented as mean  $\pm$  SEM, and a nonparametric Mann-Whitney test was performed on the data. \**P* 0.05; \*\**P* 0.01; \*\*\**P* 0.001. *N* = 6 mice per group (one-half females, one-half males).

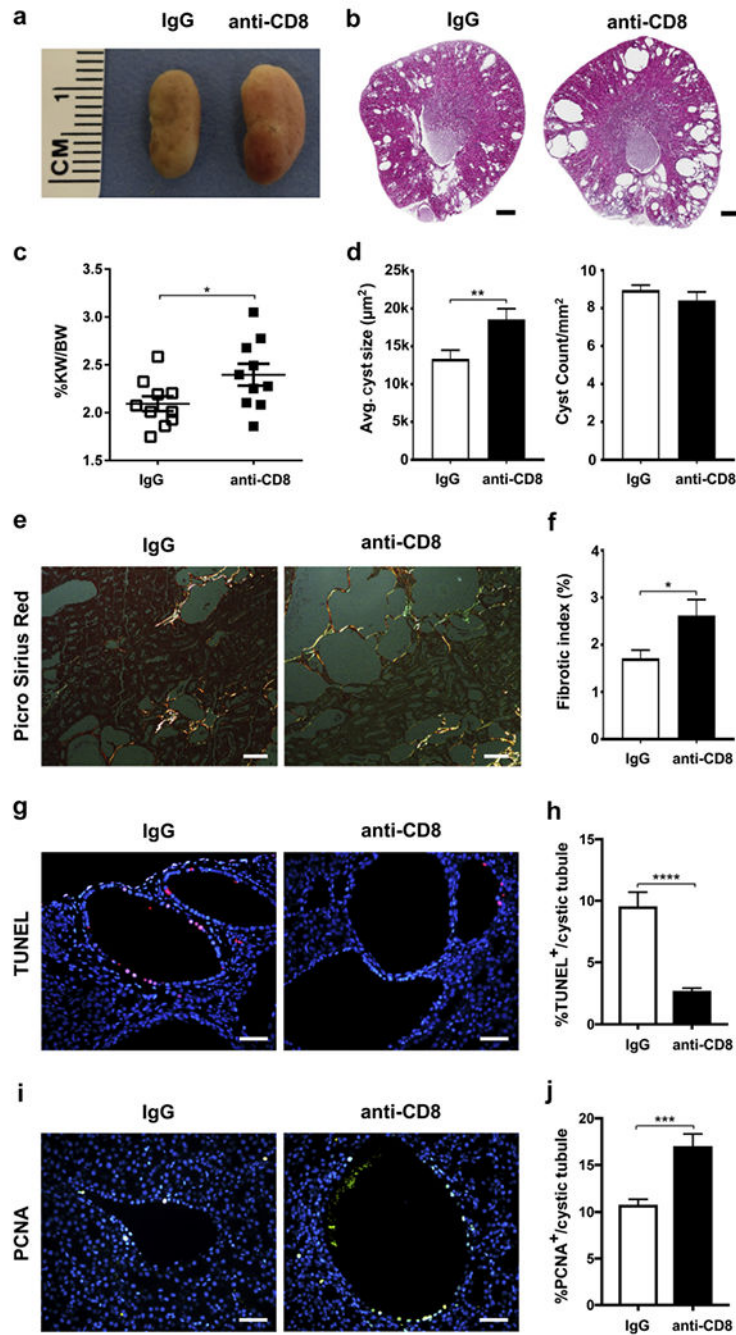


**Figure 6. CD8<sup>+</sup> T-cell depletion exacerbates cystic disease in C57Bl/6 *Pkd1*<sup>RC/RC</sup> mice.** One-month-old C57Bl/6 *Pkd1*<sup>RC/RC</sup> mice were treated by i.p. injection weekly for 8 weeks with a CD8-depleting antibody (10 mg/kg) or IgG control. Depletion of CD8<sup>+</sup> T cells worsened cystic disease as apparent by gross anatomy/histology (**a,b**), and significantly increased percent kidney weight/body weight (%KW/BW) (**c**), average cyst size (**d**), and fibrosis (% fibrotic area/[renal area – cystic area]) (**e,f**). Although average cyst size increased, cyst count remained unchanged between the treated and control groups (**d**), indicating that CD8<sup>+</sup> T cells are important in cyst progression but not initiation. (**e**)

Representative images of Picro Sirius red-stained renal histology sections visualized under polarized light to highlight collagen fibers. **(g,h)** In line with CD8<sup>+</sup> T-cell-mediated cytotoxicity, terminal deoxynucleotidyltransferase-mediated dUTP nick end-labeling (TUNEL) staining revealed a significant decrease in apoptotic epithelial cell numbers within dilated/cystic tubules of anti-CD8 treated animals versus IgG control, suggesting that programmed cell death is an essential mechanism through which CD8<sup>+</sup> T cells control cyst growth **(g)**, representative images of immunofluorescent [IF] TUNEL staining, TUNEL = red, 4',6-diamidino-2-phenylindole [DAPI] = blue). **(i,j)** Concurrent with the *in vitro* results that interferon (IFN)- $\gamma$  reduces epithelial proliferation (Figure 4), dilated/cystic tubules of anti-CD8 treated C57Bl/6 *Pkd1*<sup>RC/RC</sup> mice have significantly higher numbers of proliferating cell nuclear antigen (PCNA) positive epithelial cells versus IgG control. **(i)**, Representative images of IF PCNA staining, PCNA = green, DAPI = blue.) Bars = 500  $\mu$ m **(b)**, 100  $\mu$ m **(e)**, and 50  $\mu$ m **(g,i)**. Data are represented as mean  $\pm$  SEM, and a nonparametric Mann-Whitney test was performed on the data. \**P* 0.05; \*\**P* 0.01; \*\*\**P* 0.001; \*\*\*\**P* 0.0001. **(c,d,f)** *N* = 10 mice per group (5 females, 5 males), **(h,j)** *N* = 3 mice per group. To optimize viewing of this image, please see the online version of this article at [www.kidney-international.org](http://www.kidney-international.org).

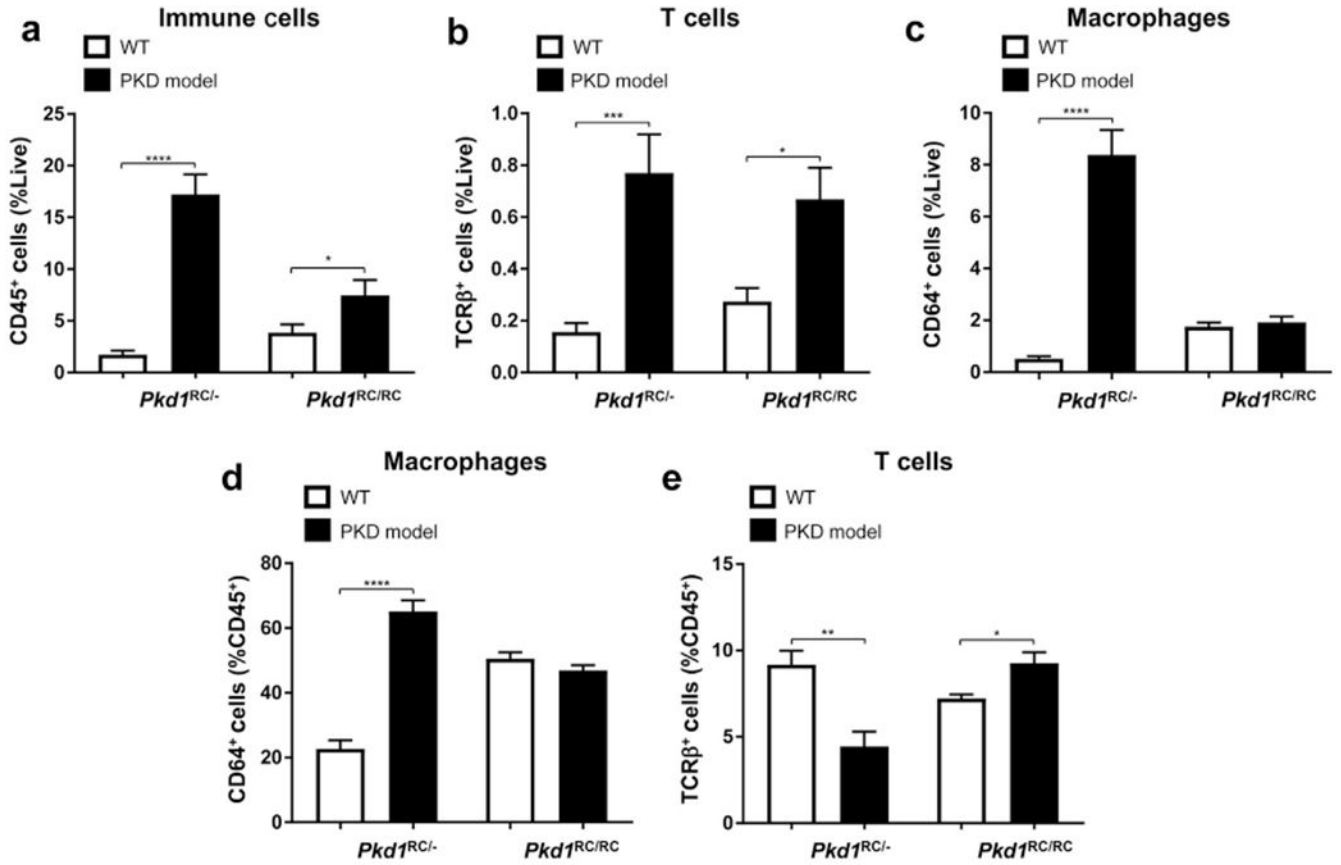


**Figure 7. In a rapidly progressive autosomal dominant polycystic kidney disease (ADPKD) model, macrophages predominantly account for the rise in immune cells associated with disease.** Both C57Bl/6 *Pkd1<sup>RC/-</sup>* mice (postnatal [P] 20) and *Pkd1<sup>RC/RC</sup>* mice (3 months) presented with an increase in CD45<sup>+</sup> cells compared with wild type (WT); however, the fold increase is more pronounced in the rapidly progressive disease (a). Although T-cell numbers increase in both models (b), the increase in macrophage numbers account for the majority of the increase in CD45<sup>+</sup> cells in the *Pkd1<sup>RC/-</sup>* model (c,d,e). Thus these data indicate that the microenvironment in the *Pkd1<sup>RC/-</sup>* model is highly inflamed, with macrophages being likely one of the key players in disease progression. Further, the adaptive and innate immune system may have a different interplay and role in cystogenesis in the rapid versus slow model of ADPKD. Data are represented as mean ± SEM, and a nonparametric Mann-Whitney test was performed on the data. \**P* 0.05; \*\**P* 0.01; \*\*\**P* 0.001; \*\*\*\**P* 0.0001. *N* = 8 mice per group (one-half females, one-half males).